International Journal of Thermal Sciences 48 (2009) 1196–1205

Contents lists available at ScienceDirect

International Journal of Thermal Sciences

www.elsevier.com/locate/ijts

Application of response surface methodology in describing the thermal performances of a pin-fin heat sink

Ko-Ta Chiang *, Chih-Chung Chou, Nun-Ming Liu

Department of Mechanical Engineering, Hsiuping Institute of Technology, No. 11, Gungye Rd., Dali City, Taichung, Taiwan 41280, R.O.C.

ARTICLE INFO

Article history:
Received 7 June 2008
Received in revised form 25 October 2008
Accepted 25 October 2008
Available online 22 November 2008

Keywords:
Response surface methodology
Optimization
Pin-fin heat sink
Central composite design

ABSTRACT

The heat sink of pin-fin array structure is widely applied in the cooling enhancement of current electronic equipment because of the advantage of non-sensitive to airflow direction and large surface area per given volume. In this study, a systematic experimental design based on the response surface methodology (RSM) is used to identify the effects of design parameters of the pin-fin heat sink (PFHS) on the thermal performance. Various design parameters, such as the height and diameter of pin-fin and the width of pitch between fins, are explored in the experiment. The thermal resistance R_{th} and pressure drop ΔP are adopted as the thermal performance characteristics. A standard RSM design called a central composite design (CCD) is applied in this experimental plan. The results distinguish the significant influential factors for minimizing the thermal resistance R_{th} and pressure drop ΔP. An effective procedure of response surface methodology (RSM) has been established for predicting and optimizing the thermal resistance R_{th} and the pressure drop ΔP of PFHS with the design constraints. The experimental results also indicate that the model proposed in this study is reasonable and accurate and can be used for describing the thermal resistance R_{th} and pressure drop ΔP with the limitations of the factors studied.

© 2008 Elsevier Masson SAS. All rights reserved.

1. Introduction

In recent years, the design and manufacture of electronic components are heading in the direction of "light, thin, short and small" under the trend of the development and advancement of electronic industry. Especially, the direction of manufacturing technology of the chips is based on the principles of "enhancing the integration density" and "curtailing the coil wire of crystal distance" in order to improve their processing speed and calculating function. But the circuit density and power dissipation of integrated circuit chips are rapidly increasing with promoting the high heat capacity within these chips. The accumulation of large amount of heat flux can easily create considerable quantities of heat stress on the chips, substrate, and their package. Therefore, the development of the efficient heat exchanger is necessary to maintain the operating temperature of electronic components at a satisfactory level. The heat sink module is the most common heat exchanger and has been extensively used in order to provide cooling function for electronic components. The heat sink module adopts the forced-air cooling technique, based on the heat diffusion between the electronic package and the ambient air. If there is an appropriate and efficient heat sink design, it will greatly affect the reliability and life span of the chip function. Many investigations of the optimum design parameters and the selection of heat sink module have been proposed in order to offer a high-performance heat removal characteristic [1–7]. Ellison [1], Kraus and Bar-Cohen [2] presented fundamentals of heat transfer and hydrodynamics characteristics of heat sinks including the efficiency of the fin, forced convective correlations, and applications in heat sinks, etc. Iyengar and Bar-Cohen [3] determined the least-energy optimization of plate fin heat sinks in the status of forced convection. Park et al. [4,5] performed the numerical optimization of the shape of a heat sink with pin-fins to improve the cooling efficiency. Park and Moon [6] proposed the progressive quadratic response surface model to obtain the optimal values of design variables for a plate-fin type heat sink. Yakut et al. [7] investigated the effects of design parameters on the heat transfer and pressure drop characteristic of a heat exchanger using the Taguchi experimental design method.

From investigations mentioned above, the optimal design and the selection of efficient heat sink module are becoming the primary challenges in the electronic industry. In order to achieve an optimum design, most attentions have focused on the parametric characteristics that influence the air flow and thermal performance. Among numerous existing designs of heat-sink modules, the design of heat sink with the pin-fin array is widely applied in the cooling enhancement of current electronic equipment. Because of the advantage of non-sensitive to airflow direction and a large surface area per given volume, various designs of pin-fin heat sink (PFHS) are manufactured to fit the certain cooled component in electronic and computer industry. In this study, a systematic

* Corresponding author.
E-mail addresses: kota@mail.hit.edu.tw, vgear2004@yahoo.com.tw (K.-T. Chiang).

1290-0729/$ – see front matter © 2008 Elsevier Masson SAS. All rights reserved.
doi:10.1016/j.ijthermalsci.2008.10.009

Nomenclature

a_i	linear effect of x_i
a_{ii}	quadratic effect of x_i
a_{ij}	linear-by-linear interaction between x_i and x_j
D	pin diameter
f	response function (or response surface)
H	pin height
L	length of heat sink base
N	number of pin fin
W	width of heat sink base
P_{in}	average pressure in the inlet of test section
P_{out}	average pressure in the outlet of test section
ΔP	pressure drop
Q	heat dissipation produced by the heating unit
R_{th}	thermal resistance
$S1$	longitudinal pitch
$S2$	transverse pitch
T_{in}	temperature in the inlet of test section
$T_{\max}$	highest temperature of heat sink base tested
t	thickness of heat sink base
W	heat dissipation produced by the heating unit
$x_1, x_2, x_3, \ldots x_n$	independent input variables
y	desired response
Greek letters	
ρ	density
ε	fitting error

experimental design based on the response surface methodology (RSM) is used to study the effects of design parameters of the pin-fin heat sink (PFHS) on the cooling efficiency. The RSM relates to the regression analysis and the statistical design of experiments for constructing the global optimization [8]. It is one of the most widely used methods to solve the optimization problem in the manufacturing environments [9–12]. In addition, the present study will apply the quadratic model of RSM associated with a sequential approximation optimization (SAO) method in order to establish an effective optimal procedure for optimizing the design parameters of PFHS under the constraints of the mass and space limitation. To achieve the high thermal performance (or cooling efficiency) under the given design constraint, the predictive model for thermal performance characteristics will be created by using the RSM.

2. Response surface methodology

The RSM is an empirical modeling approach for determining the relationship between various design parameters and responses with the various desired criteria and for searching the significance of these design parameters on the responses. It is a sequential experimentation strategy for building and optimizing the empirical model. Therefore, RSM is a collection of mathematical and statistical procedures that are useful for the modeling and analysis of problems in which response of demand is affected by design parameters and the objective is to optimize the design parameters on the desired value of the response function [8]. Through using the design of experiments and applying regression analysis, the modeling of the desired response to the several independent input variables can be gained. In the RSM, the quantitative form of relationship between desired response and independent input variables could be represented as

$$y = f(x_1, x_2, x_3, \ldots x_n) \pm \varepsilon \tag{1}$$

where y is the desired response, f is the response function (or response surface), $x_1, x_2, x_3, \ldots x_n$ are the independent input variables, and ε is the fitting error.

The appearance of response function is a surface as plotting the expected response f. The identification of suitable approximation of f will determine whether the application of RSM is successful or not. The necessary data for building the response models are generally collected by the design of experiments. In this study, the collection of experimental data adopts the face centered CCD and the approximation of f will be proposed by using the fitted second order polynomial regression model which is called the quadratic model. The quadratic model of f can be written as follows:

$$f = a_0 + \sum_{i=1}^{n} a_i x_i + \sum_{i=1}^{n} a_{ii} x_i^2 + \sum_{i<j}^{n} a_{ij} x_i x_j + \varepsilon \tag{2}$$

where a_i represents the linear effect of x_i, a_{ii} represents the quadratic effect of x_i and a_{ij} reveals the linear-by-linear interaction between x_i and x_j. Then response surface f contains the linear terms, squared terms and cross product terms. Using the quadratic model of f in this study is not only to investigate the entire factor space, but also to locate the region of desired target where the response approaches its optimum or near optimal value. The RSM is a sequential procedure and its procedure for determining the design parameters with optimal performance characteristic, including seven steps, is summarized in the following:

(1) Defining the independent input variables and desired responses with the design constraints.
(2) Adopting the face centered CCD to plan the experimental design.
(3) Performing the regression analysis with the quadratic model of response surface f.
(4) Calculating the statistical analysis of variance (ANOVA) for the independent input variables and finding which parameter significantly affects the desired responses.
(5) Determining the situation of the quadratic model of response surface f and deciding whether the model of RSM needs screening variables or not.
(6) Obtaining the optimal design parameters with the design constraints.
(7) Conducting confirmation experiment and verifying the optimal design parameters settings.

3. Experimental detail

3.1. Experimental apparatus

The experimental apparatus for exploring the thermal performance of a fan-driven pin-fin heat sink consists of air blower, pre-heater, adjustable contraction zone, honeycomb, airflow channel, test section, and measurement facilities and is schematically illustrated in Fig. 1(A). The airflow is generated with the centrifugal blower and then passes through an insulated chamber. The pre-heater controls the air temperature at inlet of the airflow channel. After the chamber, the apparatus of adjustable contraction zone and honeycomb are utilized to adjust the status of airflow to laminar flow. The airflow channel is made of a cannular cylinder and mounted in a vertical position on the top of the test section. This structure is designed to simulate the electric micro-fan (an external wing diameter of 65 mm and a motor diameter of 25 mm) installed over the heat sink. The static pressure in airflow channel is measured by using a static-pressure tapping located within

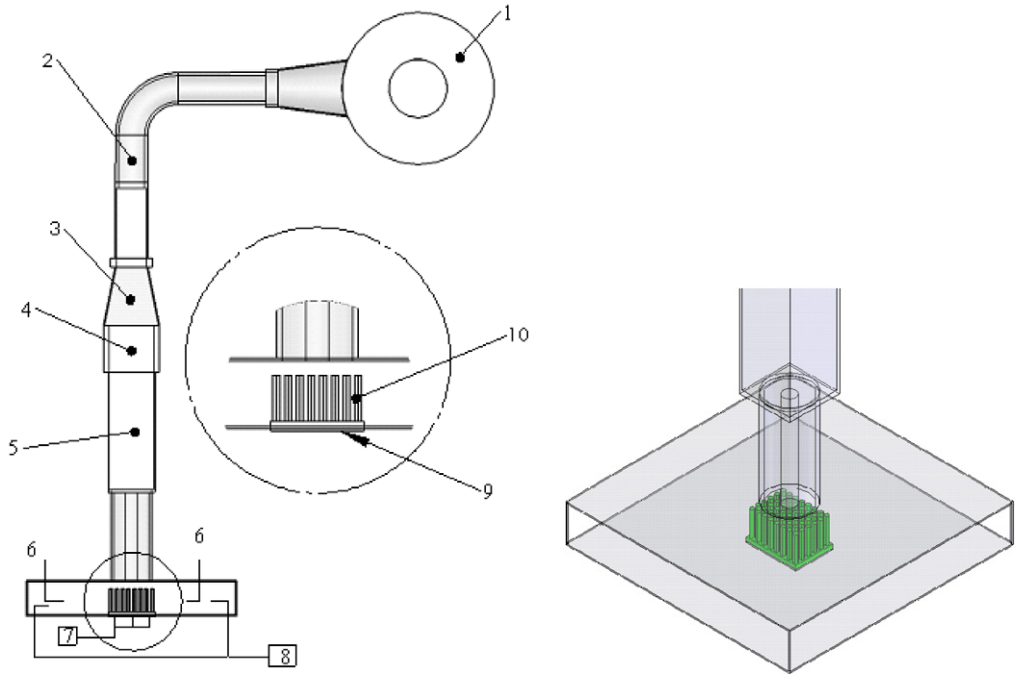

1. Blower	6. Pitot tube
2. Preheat	7. Hot-wire sensor
3. Chamber	8. Thermocouple sensor
4. Adjustable contraction zone	9. Heating unit (DC power supply)
5. Honeycomb	10. Heat sink

Fig. 1. A Schematic display of the experimental set-up.

the middle of this channel. The pressure tapping is connected to an inclined manometer.

The test section in Fig. 1(B) is constructed by a hollow rectangular block (720 × 720 × 150 mm) made up of upper and bottom plates. It is made of Plexiglas plate of 20 mm thickness. Air can be exhausted through the horizontal around of test section. The outsides of the airflow channel and the test section are insulated with a layer of glass–wool insulation. The outlet temperature of the air stream located in the horizontal around of test section is measured with thermocouple and data acquisition system. The static-pressure tapping measures the static pressure of an air stream exhausted from the horizontal around of test section. The heating unit located in the middle of the bottom plate consists of the electric heater, voltage transformer, the firebrick of 25 mm thickness and the thermal insulation. The electric heater and voltage transformer are used to control the heat flux along the bottom of base plate. The heat generated by heating unit is conducted through the heat sink at first and then it is diffused to the environment by means of forced convection at the fin-air interfaces.

The commercial extruded PFHS having a 9 × 8 array of circular pin is studied in this experiment, and its schema is shown in Fig. 2. Its material is the aluminum alloy 6063-T5 (thermal conductivity 209 W/m K). The PFHS has 60 × 54 × 6 mm base size, which is suitably mounted on the CPU board. The heat sink tested is mounted on the heating unit with two small tapped holes in the base of the heat sink. The base of PFHS is subjected to a heat load of 40 W. The temperature of PFHS base on the steady state is measured by using the twenty-five gauges (0.12 mm diameter wire) copper-constantan thermocouple installed on the base plate. The temperature data is on-line recorded using a data acquisition and calibrated to within ±0.1 °C.

3.2. Performance characteristics

Improvement of thermal performance for a fan-driven heat sink can be achieved by increasing the heat transfer rate and by promoting the capacity of fan. But, under a given operating condition of a fan, increasing the heat transfer rate is a principal cause of high thermal performance (or cooling efficiency). The important index of heat transfer rate is thermal resistance R_{th}, which is regarded as the thermal performance characteristics and is defined as

$$R_{th} = \frac{T_{max} - T_{in}}{Q} \tag{3}$$

where T_{max} is the highest temperature of heat sink base tested, T_{in} is the temperature in the inlet of test section and Q is the heat dissipation produced by the heating unit. Furthermore, the pressure drop ΔP through heat sink tested is also regarded as the thermal performance characteristics because it affects the amount of airflow through the test section or the status of bypass effect. The difference of pressure in air-flow channel and the horizontal around of test section acquires the quantity of pressure drop, which is defined in the following:

$$\Delta P = P_{in} - P_{out} \tag{4}$$

where P_{in} and P_{out} are the average pressure in the inlet and the outlet of test section, respectively. For a fan-driven heat sink, the high thermal performance (or cooling efficiency) can be obviously achieved when the thermal resistance and the pressure drop are minimized simultaneously. Both the performance characteristics are the smaller-the-better characteristics and they influence each other relatively.

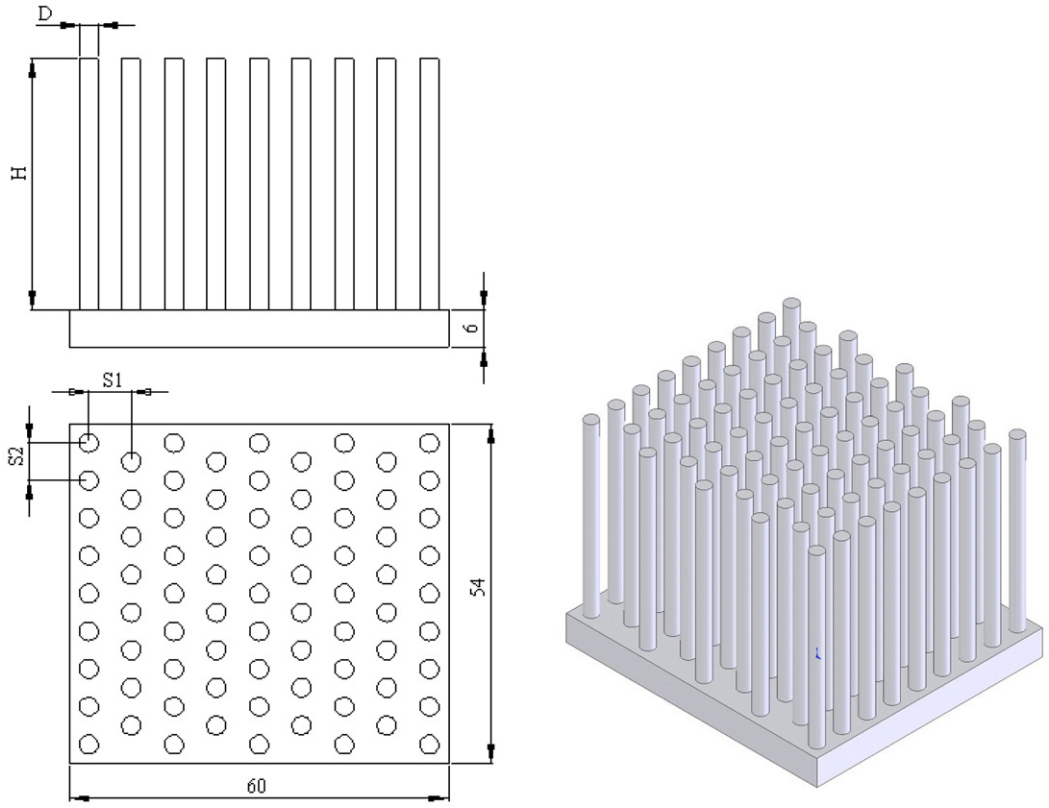

Fig. 2. Designed geometry and dimensions of pin-fin heat sink (PFHS).

Table 1
The scheme of design parameters and their levels.

Symbol	Factor	Unit	Levels	
			Low (−1)	High (+1)
A	Pin height, *H*	mm	45	60
B	Pin diameter, *D*	mm	3	5
C	Longitudinal pitch, *S1*	mm	5	8
D	Transverse pitch, *S2*	mm	5	8

3.3. Experimental conditions and plan

The geometric parameters which strongly influence the thermal performance of the heat sink are the pin height H, pin diameter D, and longitudinal pitch $S1$ and transverse pitch $S2$ of pin-fin. In this study, these parameters are chosen as the design variables. The settings of experimental plan affecting heat transfer capacity of heat sink tested are determined by a standard RSM design called a central composite design (CCD). The factorial portion of CCD is a full factorial design with all combinations of the factors at two levels (high, +1 and low, −1) and composed of the eight star points, and the six central points (coded level 0) which are the midpoint between the high and low levels. The star points are at the face of the cube portion on the design which corresponds to an α value of 1 and this type of design is commonly called the face centered CCD. Table 1 shows the levels of various design parameters and their designation. In Table 1, the total number of pin-fin is restricted to be 77 and the velocity of airflow is set at 2.5 m/s. In this experiment, 30 experiments were conducted at the stipulated conditions based on the face centered CCD. The response variables investigated are the thermal resistance R_{th} and the pressure drop ΔP. Each combination of experiments will be repeated three times under the same conditions at different times to acquire a more accurate result in this process.

Table 2
Design of experimental matrix and results for the PFHS performance characteristics.

Exp. no.	Design parameters				Experimental results	
	A Fin height	B Pin diameter	C Longitudinal pitch	D Transverse pitch	Thermal resistance R_{th} (°C/W)	Pressure drop ΔP (Pa)
1	45	3	5	5	0.2378	25.65
2	60	3	5	5	0.1932	25.01
3	45	5	5	5	0.2329	25.83
4	60	5	5	5	0.1909	26.43
5	45	3	8	5	0.2239	23.42
6	60	3	8	5	0.1879	22.33
7	45	5	8	5	0.2069	23.23
8	60	5	8	5	0.1832	23.86
9	45	3	5	8	0.2214	22.14
10	60	3	5	8	0.1983	22.37
11	45	5	5	8	0.2119	22.73
12	60	5	5	8	0.1839	22.93
13	45	3	8	8	0.2139	21.93
14	60	3	8	8	0.1879	21.33
15	45	5	8	8	0.1922	21.76
16	60	5	8	8	0.1719	21.45
17	45	4	6.5	6.5	0.2211	21.65
18	60	4	6.5	6.5	0.1867	21.21
19	52.5	3	6.5	6.5	0.2103	21.57
20	52.5	5	6.5	6.5	0.2019	22.73
21	52.5	4	5	6.5	0.2124	23.78
22	52.5	4	8	6.5	0.1923	21.77
23	52.5	4	6.5	5	0.2102	23.56
24	52.5	4	6.5	8	0.1988	22.42
25	52.5	4	6.5	6.5	0.2089	21.63
26	52.5	4	6.5	6.5	0.2109	21.83
27	52.5	4	6.5	6.5	0.2029	21.73
28	52.5	4	6.5	6.5	0.2019	21.23
29	52.5	4	6.5	6.5	0.2069	21.83
30	52.5	4	6.5	6.5	0.2029	21.33

Table 3
ANOVA table for the thermal resistance (before elimination).

Source	Sum of squares	Degrees of freedom	Mean square	f-Value	Prob. > F	
Model	0.006504	14	0.000464	39.6551	< 0.0001	significant
A	0.004296	1	0.004296	366.7432	< 0.0001	
B	0.000543	1	0.00054	46.3823	< 0.0001	
C	0.000835	1	0.000835	71.2756	< 0.0001	
D	0.000417	1	0.000417	35.6449	< 0.0001	
A^2	2.947E–06	1	2.947E–06	0.25161	0.6232	
B^2	3.327E–06	1	3.327E–06	0.2840	0.6019	
C^2	1.773E–05	1	1.774E–05	1.5141	0.2374	
D^2	5.642E–07	1	5.642E–07	0.0481	0.8293	
AB	1.540E–05	1	1.540E–05	1.3149	0.2695	
AC	6.280E–05	1	6.280E–05	5.3608	0.0352	
AD	0.000149	1	0.000149	12.7564	0.0028	
BC	5.005E–05	1	5.005E–05	4.2725	0.0564	
BD	6.683E–05	1	6.683E–05	5.7043	0.0305	
CD	6.806E–07	1	6.806E–07	0.0580	0.8128	
Residual	0.000175	15	1.171E–05			
Lack of fit	0.000106	10	1.069E–05	0.7765	0.6580	not significant
Pure error	6.883E–05	5	1.376E–05			
Cor. total	0.006679	29				
Standard. deviation = 0.003422			$R^2 = 0.973692$			
Mean = 0.20354			R^2 Adjusted = 0.949138			
Coefficient of variation = 1.681643			Predicted $R^2 = 0.874899$			
Predicted residual error of sum of squares (PRESS) = 0.000835			Adequate precision = 26.915887			

Table 4
ANOVA table for the thermal resistance (after backward elimination).

Source	Sum of squares	Degrees of freedom	Mean square	f-Value	Prob. > F	
Model	0.006371	7	0.000910	64.9817	< 0.0001	significant
A	0.004296	1	0.004296	306.7315	< 0.0001	
B	0.000543	1	0.000543	38.7926	< 0.0001	
C	0.000835	1	0.000835	59.6125	< 0.0001	
D	0.000417	1	0.000417	29.8122	< 0.0001	
AC	6.280E–05	1	6.280E–05	4.48368	0.0458	
AD	0.0001491	1	0.000149	10.6690	0.0035	
BD	6.683E–05	1	6.683E–05	4.7709	0.0399	
Residual	0.000308	22	1.400E–05			
Lack of fit	0.000239	17	1.407E–05	1.0226	0.5408	not significant
Pure error	6.883E–05	5	1.376E–05			
Cor. total	0.006679	29				
Standard. deviation = 0.003742			$R^2 = 0.953866$			
Mean = 0.20354			R^2 adjusted = 0.939187			
Coefficient of variation = 1.838805			Predicted $R^2 = 0.897901$			
Predicted residual error of sum of squares (PRESS) = 0.000682			Adequate precision = 33.706024			

4. Results and discussion

The results of the thermal performance evaluation of PFHS in each experimental plan are given in Table 2. In order to test the fit of the quadratic model with the experimental data obtained in this study, the test for significance of the regression model, the test for significance on individual model coefficients and test for lack-of-fit need to be performed [8]. The analysis of ANOVA is usually applied to summarize the above tests performed.

4.1. ANOVA analysis

The results of the quadratic model for the thermal resistance R_{th} in the form of ANOVA are presented in Table 3. The value of "Prob. > F" for this model in Table 3 is less than 0.05 (i.e. $\alpha = 0.05$, or 95% confidence). This indicates that the model is considered to be statistically significant, which is desirable as it demonstrates that the terms in the model have a significant effect on the response. In the same manner, the main effect of factor A (pin height H), factor B (pin diameter D), factor C (longitudinal pitch $S1$), factor D (transverse pitch $S2$), interaction effect of factor A (pin height H) with factor C (longitudinal pitch $S1$), interaction effect of factor A (pin height H) with factor D (transverse pitch $S2$), and interaction effect of B (pin diameter D) with factor D (transverse pitch $S2$) are the significant model terms. From the results obtained above, the significant influence of main effect and the interaction effect of factor A (pin height H) and factor B (pin diameter D) have clearly explained that the thermal removal capacity of heat sink primarily comes from the quantity of removal heat surface of heat sink module under the constant air flow velocity provided by the electric fan. Other model terms cannot be regarded as significant effect due to their "Prob. > F" value greater than 0.05. These insignificant model terms can be removed and the test of lack-of-fit also displays to be insignificant.

The backward elimination process to adjust the quadratic model of thermal resistance R_{th} eliminates the insignificant terms. The resulting ANOVA table of the reduced quadratic model for the thermal resistance R_{th} is presented in Table 4. The results from the reduced model reveal that this model is still significant in the status of the value of "Prob. > F" less than 0.05, and the test of lack-of-fit is also insignificant due to their "Prob. > F" value still greater than 0.05. The other important coefficient R^2 in the result-

Table 5
ANOVA table for the pressure drop (before elimination).

Source	Sum of squares	Degrees of freedom	Mean square	f-Value	Prob. > F	
Model	60.124010	14	4.294572	25.6254	< 0.0001	significant
A	0.056672	1	0.056672	0.3382	0.5695	
B	1.274672	1	1.274672	7.6059	0.0147	
C	12.466689	1	12.466689	74.3878	< 0.0001	
D	23.415606	1	23.415606	139.7192	< 0.0001	
A^2	0.013933	1	0.013933	0.0831	0.7770	
B^2	1.083461	1	1.083461	6.4649	0.0225	
C^2	1.134307	1	1.134307	6.7683	0.0200	
D^2	0.802865	1	0.802865	4.7906	0.0448	
AB	0.493506	1	0.493506	2.9447	0.1067	
AC	0.294306	1	0.294306	1.7561	0.2049	
AD	0.009506	1	0.009506	0.0567	0.8150	
BC	0.068906	1	0.068906	0.4112	0.5311	
BD	0.127806	1	0.127806	0.7626	0.3963	
CD	2.881506	1	2.881506	17.1937	0.0009	
Residual	2.513857	15	0.167590			
Lack of fit	2.205524	10	0.220552	3.5765	0.0861	not significant
Pure error	0.308333	5	0.061667			
Cor. total	62.637867	29				

Standard. deviation = 0.409378 — $R^2 = 0.959867$
Mean = 22.583333 — R^2 adjusted = 0.922409
Coefficient of variation = 1.812745 — Predicted $R^2 = 0.803377$
Predicted residual error of sum of squares (PRESS) = 12.316055 — Adequate precision = 18.907854

Table 6
ANOVA table for the pressure drop (after backward elimination).

Source	Sum of squares	Degrees of freedom	Mean square	f-Value	Prob. > F	
Model	59.059372	7	8.437053	51.8696	< 0.0001	significant
B	1.274672	1	1.274672	7.8364	0.0105	
C	12.466688	1	12.466688	76.6431	< 0.0001	
D	23.415605	1	23.415605	143.9554	< 0.0001	
B^2	1.108870	1	1.108870	6.8171	0.0160	
C^2	1.162735	1	1.162735	7.1483	0.0139	
D^2	0.812509	1	0.812509	4.9951	0.0359	
CD	2.881506	1	2.881506	17.7150	0.0004	
Residual	3.578493	22	0.162658			
Lack of fit	3.270160	17	0.192362	3.1193	0.1063	not significant
Pure error	0.308333	5	0.061666			

Standard. deviation = 0.403309 — $R^2 = 0.942870$
Mean = 22.583333 — R^2 adjusted = 0.924692
Coefficient of variation = 1.785873 — Predicted $R^2 = 0.866215$
Predicted residual error of sum of squares (PRESS) = 8.379956 — Adequate precision = 24.337931

ing ANOVA table is defined as the ratio of the explained variation to the total variation and is a measure of the degree of fit. When R^2 approaches to unity, the better response model fits the actual data. The value of R^2 calculated in Table 4 for this reduced model is over 0.95 and reasonably close to unity, which is acceptable. It denotes that about 95% of the variability in the data is explained by this model. It also confirms that this model provides an excellent explanation of the relationship between the independent factors and the response (thermal resistance R_{th}). Furthermore, the value of adequate precision in this model, which compares the range of the predicted value at the design point to the average prediction error, is well above 4. The value of ratio is greater than 4, which presents the adequate model discrimination.

The same procedure is applied to deal with the other response, pressure drop ΔP, and the resulting ANOVA for the quadratic model is shown in Table 5. The value of "Prob. > F" in Table 5 for this model is also less than 0.05 (i.e. $\alpha = 0.05$, or 95% confidence) indicates that the model is considered to be statistically significant. The significant model terms include the main effect of factor B (pin diameter D), factor C (longitudinal pitch $S1$), factor D (transverse pitch $S2$), second order effect of factor B (pin diameter D), factor C (longitudinal pitch $S1$), factor D (transverse pitch $S2$), and interaction effect of factor C (longitudinal pitch $S1$) with factor D (transverse pitch $S2$). From the result obtained above, the significant influence of factor B (pin diameter D), factor C (longitudinal pitch $S1$) and factor D (transverse pitch $S2$) are apparently related to the status of airflow. The other model terms cannot be regarded as significant effect due to their "Prob. > F" values greater than 0.05. These insignificant model terms can be removed and the test of lack-of-fit also displays to be insignificant. Using the backward elimination process, the resulting ANOVA table of the reduced quadratic model for the pressure drop ΔP is presented in Table 6. The reduced model results reveal that the model is still significant and the test of lack-of-fit is also insignificant. The R^2-value for pressure drop is 0.93, which is close to 1. The adequate precision value of this reduced model is still well above 4.

According to the results in ANOVA, a sensitivity analysis for the design factors in the thermal resistance R_{th} and the pressure drop ΔP is performed and shown in Fig. 3. From the results of percent contribution for each significant design factor, the front two significant design factors in the thermal resistance R_{th} are factor A (pin height H) and factor B (pin diameter D), and the front two significant design factors in the pressure drop ΔP are factor C (longitudinal pitch $S1$) and factor D (transverse pitch $S2$). Factor A

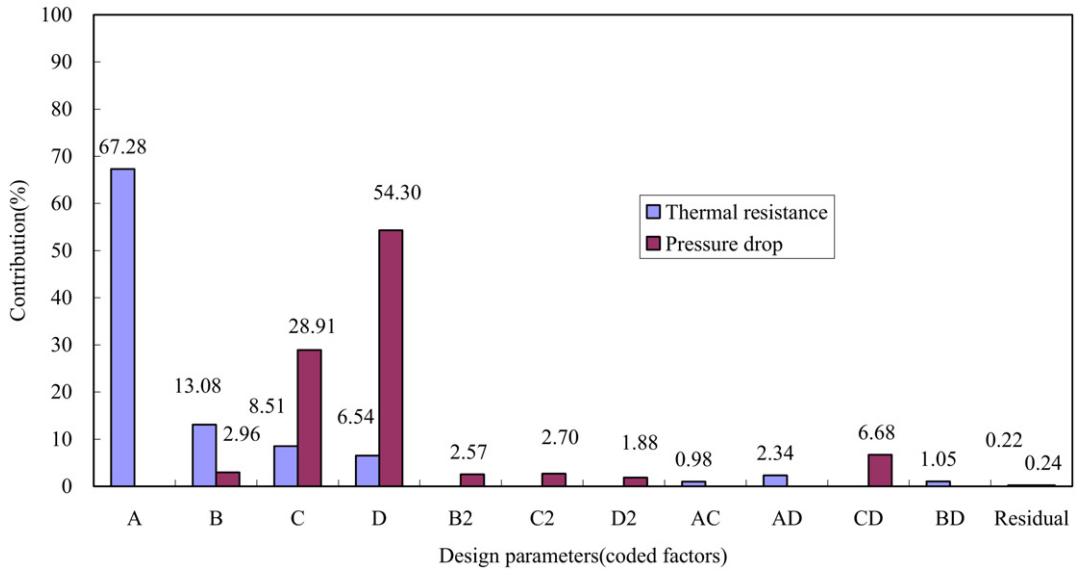

Fig. 3. The sensitivity analysis of design parameters (coded factors).

(pin height H) and factor B (pin diameter D) determine the quantity of removal heat surface of heat sink module. Factor B (pin diameter D) and factor C (longitudinal pitch $S1$) affect the status of airflow. Therefore, it is clear that the thermal resistance R_{th} is subjected to the quantity of removal heat surface of heat sink module and the pressure drop ΔP is influenced by the status of airflow.

Through the backward elimination process, the final quadratic models of response equation in terms of coded factors are presented as follows:

– Thermal resistance R_{th}

$$R_{th} = 0.20354 - 0.01545A - 0.005494B - 0.006811C - 0.004816D + 0.001981AC + 0.003056AD - 0.002043BD \quad (5)$$

– Pressure drop ΔP

$$\Delta P = 21.503333 + 0.266111B - 0.832222C - 1.1405556D + 0.625B^2 + 0.64C^2 + 0.535D^2 + 0.424375CD \quad (6)$$

In terms of actual factors, the final quadratic models of response equation are as follow:

– Thermal resistance R_{th}

$$R_{th} = 0.501433 - 0.004970H + 0.003361D - 0.013786S1 - 0.012023S2 + 0.000176HS1 + 0.000271HS2 - 0.001362DS2. \quad (7)$$

– Pressure drop ΔP

$$\Delta P = 69.020301 - 4.733888D - 5.478564S1 - 5.077453S2 - 0.625D^2 + 0.284444S1^2 + 0.237777S2^2 + 0.188611S1S2. \quad (8)$$

The model obtained above can be used to predict the thermal resistance R_{th} and pressure drop ΔP within the limits of the factors studied. The normal probability plots of the residuals for both the thermal resistance R_{th} and the pressure drop ΔP are displayed in Figs. 4 and 5, respectively. Notice that the residuals generally fall on a straight line implying that the errors are normally distributed. Further, it supports adequacy of the least-square fit.

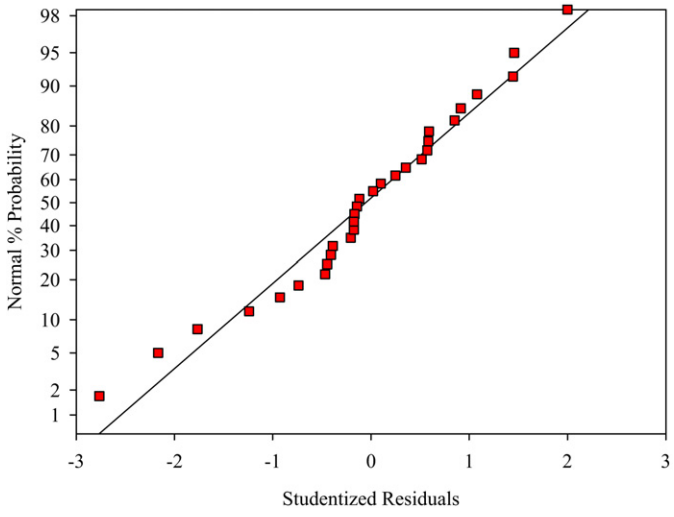

Fig. 4. Normal probability plot residuals for the thermal resistance R_{th}.

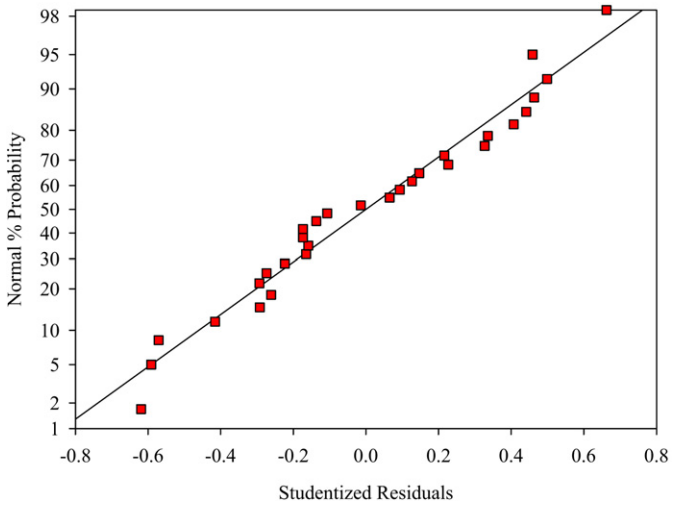

Fig. 5. Normal probability plot residuals for the pressure drop ΔP.

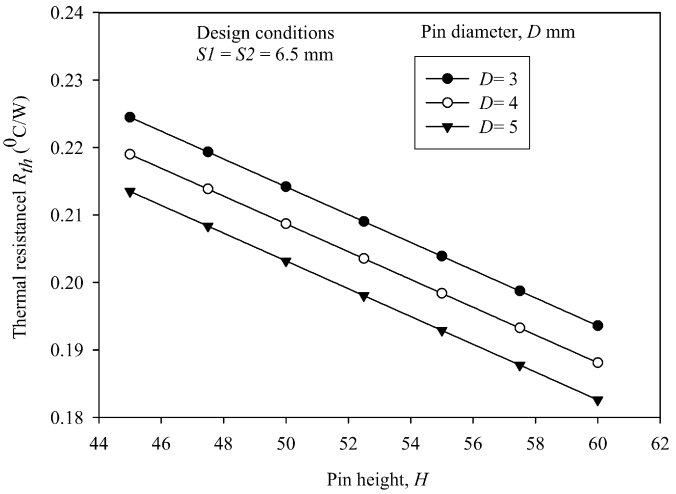

Fig. 6. The effect of pin height on the thermal resistance at different pin diameters.

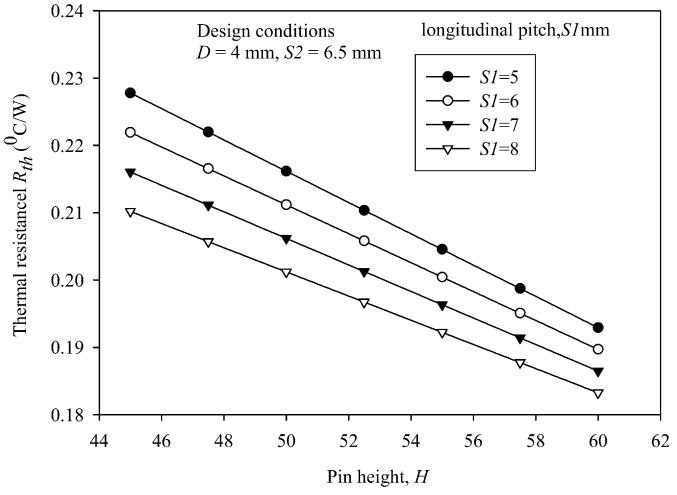

Fig. 7. The effect of pin height on the thermal resistance at different longitudinal pitch.

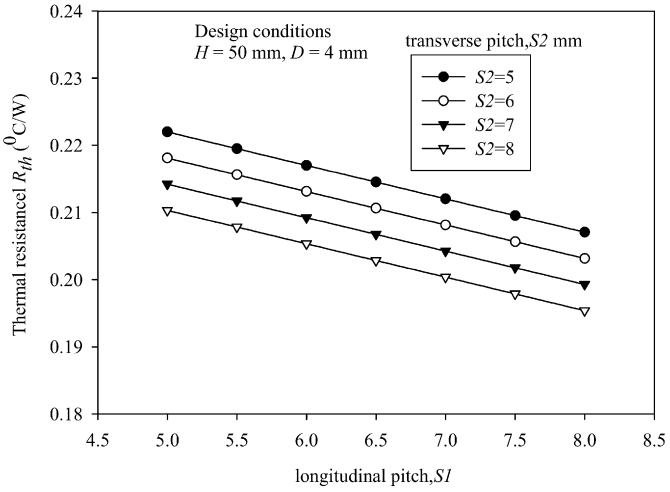

Fig. 8. The effect of longitudinal pitch on the thermal resistance at different transverse pitch.

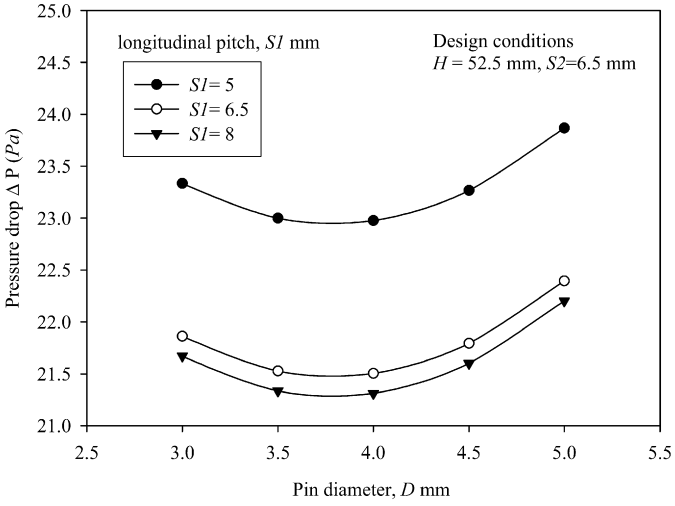

Fig. 9. The effect of pin diameter on the pressure drop at different longitudinal pitch.

4.2. Effect of design parameters on the thermal resistance

The thermal resistance R_{th} in the thermal performance of heat sink module is an important index because of its vital heat removal effect on the electronic components. The effect of pin height H on the thermal resistance R_{th} at various pin diameter D and longitudinal pitch $S1$ is presented in Figs. 6 and 7, respectively. From these figures, it has been seen that an increase in the pin height H leads to the decrease of the thermal resistance R_{th}. It has also been found that the effect of pin diameter D has the similar result. Both the height H and diameter D of pin are chiefly concerned with the quantity of removal heat surface of heat sink module. These results have been attributed to the increase of removal heat surface of heat sink module, which leads to the increase in the rate of removal heat capacity, and hence the heat sink module has lower value of thermal resistances R_{th}. In addition, the increase of the longitudinal pitch $S1$ also increases the thermal resistances R_{th}. But in Fig. 6, the decreasing rate of thermal resistance R_{th} become eased as the longitudinal pitch $S1$ increases.

The thermal performance of heat sink module not only depends on the quantity of removal heat surface, but also is subjected to the bypass air of convective effect. Under the constraint of fan capability, the geometric configuration of the heat sink module can apparently influence the status of the bypass air. Therefore, Fig. 8 shows the effect of the longitudinal pitch $S1$ and transverse pitch $S2$ on the thermal resistances R_{th}. Increasing both values of longitudinal pitch $S1$ and transverse pitch $S2$ lead to the increase of dimension of gap among all pins and subsequently strengthen the amount and the bypass effect of airflow. It is clear that the thermal resistance R_{th} generally decreases with the increase of the longitudinal pitch $S1$ and the transverse pitch $S2$ of pin.

4.3. Effect of design parameters on the thermal resistance

About the strength and weakness of heat removal capacity of heat sink module, it will be judged whether the heat capacity can be quickly brought away by using the airflow field of forced convection caused by the electric fan through the surrounding of heat sink. The pressure drop ΔP through tested heat sink module affects the amount of airflow and the status of bypass effect. Fig. 9 presents the effect of pin diameter D on the pressure drop ΔP at various longitudinal pitches. First, it has been seen that an increase in the pin diameter leads to the decrease of the pressure drop ΔP. This decrease is, however, diminished after 4 mm. This result indicates that an increase in the pin diameter causes the decrease of gap among all pins, which obstructs the amount of airflow. Hence,

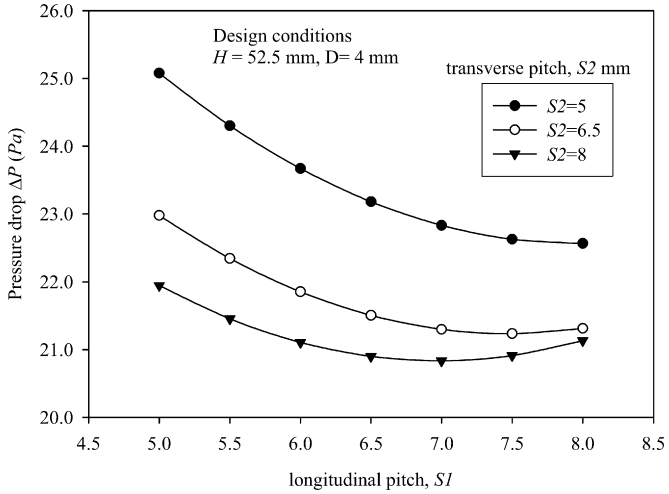

Fig. 10. The effect of longitudinal pitch on the pressure drop at different transverse pitch.

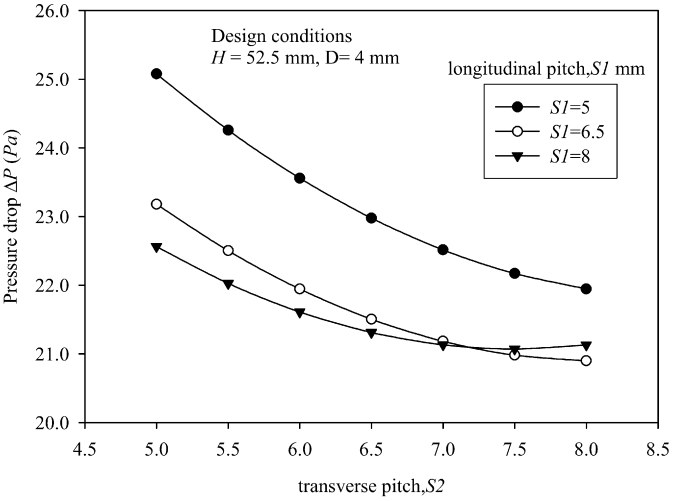

Fig. 11. The effect of transverse pitch on the pressure drop at different longitudinal pitch.

the decrease in pin diameter that lowers under a certain limit, leads to the small gap among all pins, which increases the pressure drop ΔP, and subsequently decreases the heat removal capacity of heat sink module.

Figs. 10 and 11 show the effect of longitudinal pitch *S1* and the transverse pitch *S2* on the pressure drop ΔP. The longitudinal pitch *S1* and the transverse pitch *S2* determinate the dimension of gap among all pins in the longitudinal and transverse direction, respectively. In Fig. 10, it is shown that the pressure drop ΔP generally decreases with the increase of the longitudinal pitch *S1* up to 7.0 and then increases with a further increase in the longitudinal pitch *S1*. Fig. 11 presents the above similar conditions which are especially obvious when the transverse pitch *S2* is 8 mm. Increasing both the longitudinal pitch *S1* and the transverse pitch *S2* lead to the generation of higher amount of airflow, which is subjected to the dimension of the gap among all pins. This will cause a decrease in the pressure drop ΔP and strengthen the airflow field of forced convection resulting from the high heat removal capacity. Furthermore, the value of the pressure drop ΔP is decreasing continuously with the increase of the dimension of gap among all pins until reaching a situation in which the bypass effect will have no more increase.

Table 7
The initial and optimum designing values.

Parameters	Unit	Initial value	Optimal value
Fin height, *H*	mm	45	60
Pin diameter, *D*	mm	3	4.48
Longitudinal pitch, *S1*	mm	5	7.60
Transverse pitch, *S2*	mm	5	7.97
Thermal resistance R_{th}	°C/W	0.2378	0.1792
Pressure drop ΔP	Pa	25.65	21.21

4.4. Optimization of design parameters

The optimization of PFHS with the design constraints of mass and space limitation in this study is to find the optimal values of design parameters (X) for minimizing the value of thermal resistance R_{th} and pressure drop ΔP. The optimization problem can be approximated by the following equations and then solved by means of a sequential approximation optimization (SAO) method. The SAO strategy in the RSA applies the approximate procedure, which is iteratively repeated until convergence.

$$\text{Find } X = [H, D, S1, S2] \tag{9}$$

$$\text{to minimize } f(X) = R_{th} \text{ and } f(X) = \Delta P \tag{10}$$

$$\text{Subject to } 45 \leqslant H \leqslant 60 \text{ mm},\ 3 \leqslant D \leqslant 5 \text{ mm} \tag{11a}$$

$$5 \leqslant S1 \leqslant 8 \text{ mm},\ 5 \leqslant S2 \leqslant 8 \text{ mm} \tag{11b}$$

$$mass(X) \leqslant 150 \text{ g}. \tag{11c}$$

In Eq. (11c), the mass of PFHS is less than the lowest value of 150 g due to the weight load of general integrated circuit chips is constrained in this range. The correlation between mass and design parameters is defined as following:

$$Mass = \rho(N\pi/4D^2H + LWt) \tag{12}$$

where ρ is the density of material, N is the number of pin fin, L, W, and t are the length, width and thickness of heat sink base, respectively. Table 7 presents the results obtained from the four different pin-fin parameters with the optimum adjustments found by the SAO method in the RSA. As shown in Table 7, the optimized thermal resistance R_{th} of 0.1792 °C/W represents a reduction of 24.6% compared to the initial thermal resistance R_{th} of 0.2378 °C/W. Also, the optimized pressure drop ΔP is decreased to 21.21 Pa with a reduction of 17.3% compared to the initial pressure drop ΔP of 25.65 Pa.

5. Confirmation experiments

In order to verify the adequacy of the quadratic model obtained in this study, the four confirmation run experiments are performed for the thermal resistance R_{th} and the pressure drop ΔP. The data from the confirmation runs and their comparisons with the predicted values for the thermal resistance R_{th} and the pressure drop ΔP are listed in Table 8. From the analysis of Table 8, the residual and the percentage error calculated are small. The range of percentage error between the experimental and the predicted value of R_{th} and ΔP lie within −2.58 to 1.16% and −2.68 to 2.66%, respectively. All the experimental values for the confirmation run are within the 95% prediction interval. Obviously, the quadratic model obtained is excellently accurate.

6. Conclusion

The effects of design parameters of PFHS on the thermal performance have been investigated with a systematic experimental design based on the response surface methodology (RSM). In

Table 8
Confirmation experiment.

Exp. no.	Designing parameters				Thermal resistance R_{th}			Pressure drop ΔP		
	A	B	C	D	Exp.	Predicted	Error (%)	Exp.	Predicted	Error (%)
1	45	3	5	5	0.2378	0.2391	0.55%	25.65	25.43	−0.86%
2	52.5	4	6.5	6.5	0.2089	0.2035	−2.58%	21.63	21.05	−2.68%
3	60	5	8	8	0.1719	0.1739	1.16%	21.45	22.02	2.66%
4	60	4.48	7.6	7.97	0.1802	0.1792	−0.55%	21.26	21.21	−0.24%

this study, an effective procedure of response surface methodology (RSM) has been established for predicting and optimizing the thermal resistance R_{th} and the pressure drop ΔP of PFHS with the design constraints. The results can be concluded as follows:

(1) For minimizing the value of thermal resistance R_{th}, the main effect and interaction effect of pin height H and pin diameter D play the significant influence factors. Both the height H and diameter D of the pin are chiefly related to the quantity of removal heat surface of heat sink module. Increasing removal heat surface of heat sink module leads to the increase in the rate of removal heat capacity, hence the heat sink module has lower value of thermal resistances R_{th}.
(2) The effects of pin diameter D, longitudinal pitch $S1$ and transverse pitch $S2$ are clearly related to the dimension of the gap among all pins, which affects the airflow field of forced convection. The results represents that the value of the pressure drop ΔP is decreasing continuously with the increase of the dimension of gap among all pins until reaching a situation in which the bypass effect will have no more increase.
(3) Using the SAO method, the four different pin-fin parameters with the optimum adjustment are acquired and the minimal values of R_{th} and ΔP have been predicted and verified by conducting confirmation experiments. From the results of conducting confirmation experiments, the model developed by using RSM is reasonably accurate and can be used for describing thermal resistance R_{th} and pressure drop ΔP with the limits of the factors studied.

References

[1] G.N. Ellison, Thermal Computations for Electronic Equipment, second ed., Van Nostrand Reinhold Corporation, New York, 1989.
[2] A.D. Kraus, A. Bar-Cohen, Thermal Analysis and Control of Electronic Equipment, Hemisphere Publishing Corporation, Washington, 1983.
[3] M. Iyengar, A. Bar-Cohen, Least-energy optimization of forced convection plate-fin heat sinks, IEEE Trans. Components and Packaging Technologies 26 (2003) 62–70.
[4] K. Park, D.H. Choi, K.S. Lee, Optimum design of plate heat exchanger with staggered pin arrays, Numerical Heat Transfer Part A 45 (2004) 347–361.
[5] K. Park, D.H. Choi, K.S. Lee, Numerical shape optimization for high performance of a heat sink with pin-fins, Numerical Heat Transfer Part A 46 (2004) 909–927.
[6] K. Park, S. Moon, Optimal design of heat exchangers using the progressive quadratic response surface model, International Journal of Heat and Mass Transfer 42 (2005) 237–244.
[7] B. Sahin, K. Yakut, I. Kotcioglu, C. Celik, Optimum design parameters of a heat exchanger, Applied Energy 82 (2005) 90–106.
[8] R.H. Myers, D.H. Montgomery, Response Surface Methodology, John Wiley & Sons, USA, 1995.
[9] J. Grum, J.M. Slab, The use of factorial design and response surface methodology for fast determination of optimal heat treatment conditions of different Ni–Co–Mo surface layers, Journal of Material Processing Technology 155–156 (2004) 2026–2032.
[10] B. Ozcelik, T. Erzurmlu, Determination of effecting dimensional parameters on warpage of thin shell plastic parts using integrated response surface method and genetic algorithm, International Communication of Heat and Mass Transfer 32 (2005) 1085–1094.
[11] H.K. Kansal, S. Singh, P. Kumar, Parametric optimization of powder mixed electrical discharge machining by response surface methodology, Journal of Material Processing Technology 169 (2005) 427–436.
[12] H. Oktem, T. Erzurmlu, H. Kurtaran, Application of response surface methodology in the optimization of cutting conditions for surface roughness, Journal of Material Processing Technology 170 (2005) 11–16.